J Appl Electrochem (2011) 41:481–490
DOI 10.1007/s10800-011-0258-3

ORIGINAL PAPER

Effect of ionic liquid additive [BMIM]HSO_4 on zinc electrodeposition from impurity-containing sulfate electrolyte. Part I: current efficiency, surface morphology, and crystal orientations

Qibo Zhang · Yixin Hua

Received: 10 October 2010 / Accepted: 4 February 2011 / Published online: 23 February 2011

Abstract The effects of ionic liquid additive 1-butyl-3-methylimidazolium hydrogen sulfate-[BMIM]HSO_4 on the current efficiency (CE), surface morphology, and crystallographic orientations during zinc electrodeposition from acidic sulfate solutions containing some common impurities such as copper, iron, cobalt, nickel, and lead were investigated. The results indicated that all the metallic impurities studied exerted a deleterious effect on the zinc electrodeposition process by decreasing the CE, influencing the purity, and inducing changes in morphology of the cathodic deposits. The addition of [BMIM]HSO_4 was observed to relieve the harmful effects of these impurities to some extent, and led to reduce the impurity content in the zinc deposits and improve the CE and the quality of the cathodic deposits. The data obtained from X-ray diffraction revealed that the presence of these impurities alone and in combination with [BMIM]HSO_4 did not change the structure of the electrodeposited zinc but affected the crystallographic orientation of the crystal planes.

Keywords Zinc electrodeposition · Ionic liquid · Additive · Impurities · Deposit morphology · Crystal orientation

1 Introduction

Zinc electrodeposition process is extremely sensitive to the presence of certain impurities in the electrolyte. Low levels of these impurities greatly interfere in the deposition process, leading to a decrease in zinc current efficiency (CE) and to changes in deposits' morphology [1] and cathodic polarization [2, 3]. Neutral purification eliminates the bulk of the impurities, but in certain instances, their concentrations may still be high enough to cause difficulties in the zinc electrodeposition [4, 5]. Over the past few decades, the effects of numerous metallic impurities on the zinc electrodeposition have been studied in laboratory. Copper and iron can be co-deposited with zinc during the electrodeposition process and serve as micro-cathodes on which hydrogen is evolved. Copper [4, 6–8] was found to reduce the deposit grain size and facilitate zinc deposition, while iron [7, 8] inhibited zinc deposition process without inducing significant changes in deposit morphology. Cobalt and nickel [5, 6, 9–12] which were difficult to remove from the electrolyte can cause mild redissolution of the zinc deposit, but this occurred only after an induction period that was dependent on the impurity concentration and on the zinc-to-acid ratio. Lead [13] had a small beneficial effect on the CE and exerted a grain-refining effect on the cathodic deposit with changing the orientation. Cadmium [7] did not affect the growth or orientation of the zinc deposit but reduced the deposit grain size. Small concentration of germanium [6, 14, 15] and tin [16] drastically reduced the CE and induced changes in cathodic polarization, deposit morphology and crystallites orientation. Antimony [1, 2, 17–19] was recognized as one of the most deleterious impurities for zinc electrodeposition whose presence in the electrolyte produced spongy and dark deposits. To counteract the harmful effects of metallic impurities and achieve high CE and produce a smooth, leveled, and dense cathodic deposit, colloidal additives such as glue [1, 5], gelatine [8, 20], and gum arabic [21], and many organic additives [22, 23] are widely employed.

Q. Zhang (✉) · Y. Hua
Key Lab of Ionic Liquids Metallurgy, Faculty of Metallurgical and Energy Engineering, Kunming University of Science and Technology, Kunming 650093, China
e-mail: qibozhang@yahoo.com.cn

Appropriate amounts of these additives [8] were found to be necessary for obtaining fine-grained zinc deposits with good quality and high CE from impurity-containing electrolyte.

Saba and Elsherief [8] demonstrated that certain combinations of glue and foreign cations can improve the CE and obtain continuous and small-grained zinc deposits. Sider and Piron [24] studied the effects of 2-butyne-1,4-diol on the electrocrystallization process of zinc from impurity-containing electrolyte and found that this additive can counteract the harmful effects of antimony and nickel, and improve the CE and zinc deposit quality. Cachet et al. [25] found that triethylbenzylammonium chloride (TEBA) had been shown to increase the induction period which preceded the reverse dissolution of zinc deposits obtained under galvanostatic conditions in nickel-containing electrolyte. Karavasteva et al. [23, 26] have reported the influence of the combined addition of nonylphenolpolyethylene glycol,dinaphthylmethane-4,4′-disulfonic acid, and polyethylene glycol on the electrolyte with high concentrations of impurities. They found that specific combinations of these surfactants can decrease the negative effects of metal impurities on both the CE and structure of zinc deposits. Das and co-workers [19, 27–32] have studied the effects of some organic additives on the zinc electrodeposition from the antimony-containing solutions. They demonstrated that there were specific combinations of these additives and antimony, wherein maximum CE and minimum power consumption, as well as acceptable surface morphology could be achieved.

In our previous study, ionic liquid additive [BMIM]HSO_4 and its mixture with gelatine have been found to be efficient as leveling agents in zinc [20] electrodeposition. However, further study needs to be done when some industrial impurities are also present in the electrolyte to establish whether its leveling effect is still observed. The aim of this study is to investigate the effects of [BMIM]HSO_4 on the CE, surface morphology, and crystallographic orientations during zinc electrodeposition from sulfate baths containing various common metallic impurities such as, copper, iron, cobalt, nickel, and lead.

2 Experimental details

2.1 Reagents

The zinc electrolyte concentration of 55 g dm^{-3} zinc and 150 g dm^{-3} sulfuric acid was prepared from AnalaR zinc sulfate ($ZnSO_4 \cdot 7H_2O$), and analytic grade H_2SO_4, and the specific experimental procedures were similar to that described previously [20]. The purified neutral zinc sulfate solution had the following impurities in mg dm^{-3} (determined by atomic adsorption spectrometry), Mn (0.32), Fe (0.12), Cd (0.06), Cu (0.05), Ni (0.05), Co (0.03), and Pb (0.12). All foreign cations were added as the sulfate salts to the purified solution to get the preferred electrolyte composition. Ionic liquid additive [BMIM]HSO_4 was laboratory synthesized, and the specific synthetic methods were as mentioned previously [33].

2.2 Electrolysis

Small-scale galvanostatic electrolysis was performed in a rectangular flow cell containing ca. 250 mL electrolyte with dimension of 10 × 8 × 6 cm^3 made of plexiglass by chronopotentiometric measurements. The flow rate of the electrolyte was maintained at 1.2 dm^3 h^{-1} during the deposition process. A pure vertical planar aluminum (>99.95%) sheet and two parallel lead–silver–calcium–strontium alloy (Ag 0.2%, Ca and Sr 0.1–0.13%) plates with 5.0 cm^2 as effective area were used as the cathode and anode, respectively. The cathode was measured 15 × 15 mm^2 and mounted so that zinc was deposited on both sides onto a total area of 4.5 cm^2. The interelectrode distance was 2.5 cm. All the electrolysis experiments were run in a constant temperature bath at 40 ± 1 °C. In all the cases, the current density was held constant at 400 A m^{-2} during the deposition time of 2 h. After the electrolysis, the cathode was removed from the cell and washed thoroughly with distilled water and dried. The CE was calculated by weight according to Faraday's law.

2.3 Deposit examination

The impurities' contents in the zinc electrodeposits were determined by dissolving them in dilute HNO_3 and quantitatively analyzing by atomic adsorption spectrometry (Shimadzu AA6300, Japan). Sections of the zinc deposits were examined by scanning electron microscopy (SEM) using a Tescan VEGA II XMH microscope to determine the surface morphology of the deposit. A Rigaku D/max 2200 X-ray diffractometer was used for examining the preferred crystal orientations relative to ASTM standard for zinc powder.

3 Results and discussion

3.1 Current efficiency

The effects of ionic liquid additive [BMIM]HSO_4 on the CE during zinc electrodeposition from electrolytes containing various impurities such as copper, iron, cobalt, nickel, and lead were studied, and the corresponding results are given in Tables 1, 2, 3, 4, and 5. It is observed that the

CE decreases in all the cases of the electrolytes containing impurities alone except lead, and this effect is more pronounced with increasing impurity concentration. It can be seen from Fig. 1 that CE drops off much more rapidly at higher concentrations. For example, at lower concentration of 1 mg dm^{-3}, the CE does not change significantly. On increasing their concentrations to greater than 5 mg dm^{-3}, a sharp decrease in the CE by ~8% is seen for nickel-containing electrolyte, whereas slight decreases in the CE by ~0.7, 0.5, and 1.3% are observed for copper, iron, and cobalt-containing electrolytes, respectively. When the electrolytes contain 20 mg dm^{-3} nickel, cobalt, copper, iron, and lead, the CEs obtained are 59.9, 74.7, 83.5, 88.4, and 91.7%, respectively. Therefore, it can be concluded that the negative influence of these impurities on the CE at a given concentration is in the order: Ni > Co > Cu > Fe > Pb.

It is noteworthy that the addition of appropriate amounts of [BMIM]HSO_4 to the baths containing 10 mg dm^{-3} impurities increases the CE by ~1–11% in comparison to these electrolytes in the absence of additive. For instance, an increase in CE by ~11% is obtained with the addition of 5 mg dm^{-3} [BMIM]HSO_4 in the electrolyte containing 10 mg dm^{-3} nickel compared to the additive-free electrolyte. Similar results can also be observed when [BMIM]HSO_4 is introduced into the other impurity-containing electrolytes. The increase in CE in the presence of [BMIM]HSO_4 can be attributed to the suppression of the electroreduction of these impurities' ions and hydrogen evolution by blocking the active sites through its cathodic adsorption [20, 34], and consequently, inhibiting the dissolution of the deposited zinc. Another distinct change noted is that lead slightly increases the CE of zinc deposition. A CE of 92.0% is achieved with the addition of 10 mg dm^{-3} lead. Such increases in CE have also been observed by other researchers [13] and are observed generally because lead can readily co-deposit with zinc and the hydrogen overpotential on lead is higher than that on zinc, which leads to hinder the hydrogen evolution, and thus induces the zinc deposition process. The combination of 10 mg dm^{-3} [BMIM]HSO_4 and 10 mg dm^{-3} lead decreases the CE by ~2% in contrast to the additive-free solution. This decrease in CE can be attributed to the surface coverage of the cathode by a strongly adsorbed additive layer with an excess addition, which decreases the zinc deposition rate and inhibits the electroreduction of zinc.

3.2 Deposit contamination

The zinc electrodeposits obtained at different concentrations of impurities in the absence and presence of [BMIM]HSO_4 were analyzed, and the results are given in Tables 1, 2, 3, 4, and 5. The standard reduction electrode potential of zinc ion, H^+, and other metal ions of impurities in aqueous solution are reported in Table 6. From Table 6, it may be expected that, before reduction of Zn^{2+}, the reduction of these impurities is possible as the reduction of Zn^{2+} should occur at a potential more negative than the reduction of all the impurities studied. In all the cases, deposits are found to be contaminated in the presence of impurities, where their contents in zinc deposits are observed to increase with increasing impurity concentration in the electrolytes. For example, the zinc deposit obtained from the electrolyte with 5 mg dm^{-3} copper contained ~0.074% Cu. Increasing the copper concentration to 20 mg dm^{-3} increases the copper content in the zinc deposit to ~0.323%. Similar observations were also obtained for the other impurity-containing electrolytes. The extent of contamination of the zinc deposits in the presence of these impurities appears to be in the order: Cu > Pb > Fe > Ni > Co. This rule is quite different from the result exerted by their effects on the CE, which could be attributed to their action mechanism. It is unexpected that nickel and cobalt, which have more deleterious influence on the CE, have less significant effect on the purity of the zinc deposits than other impurities do. The behavior could be attributed to their periodic action mechanism. The harmful influences of nickel and cobalt on the CE could be associated with the formation of local cells whereby

Table 1 Effects of [BMIM]HSO_4 on current efficiency, cathodic contamination, and crystallographic orientations of the zinc electrodeposits obtained from copper-containing electrolytes

Copper (mg dm^{-3})	[BMIM]HSO_4 (mg dm^{-3})	Current efficiency (%)	Cathodic contamination (%)	Crystallographic orientations
0	0	90.8	–	(101) (201) (100) (112)
1	0	90.5	0.020	(101) (102) (112) (100)
2	0	90.3	0.034	(101) (103) (102) (100)
5	0	90.1	0.074	(101) (103) (102) (100)
10	0	89.5	0.185	(101) (002) (100) (110)
20	0	88.4	0.323	(101) (002) (100) (102)
10	5	90.9	0.065	(101) (002) (100) (103)
10	10	91.0	0.052	(101) (110) (102)

Table 2 Effects of $[BMIM]HSO_4$ on current efficiency, cathodic contamination, and crystallographic orientations of the zinc electrodeposits obtained from iron-containing electrolytes

Iron (mg dm^{-3})	$[BMIM]HSO_4$ (mg dm^{-3})	Current efficiency (%)	Cathodic contamination (%)	Crystallographic orientation
1	0	90.7	0.016	(101) (102) (103) (100)
2	0	90.5	0.028	(101) (102) (103)
5	0	90.3	0.054	(101) (102) (100)
10	0	90.0	0.097	(101) (112) (103) (102)
20	0	83.5	0.252	(101) (002) (102) (103)
10	5	90.9	0.030	(101) (102) (103) (100)
10	10	91.1	0.021	(101) (102) (112) (103)

Table 3 Effects of $[BMIM]HSO_4$ on current efficiency, cathodic contamination, and crystallographic orientations of the zinc electrodeposits obtained from nickel-containing electrolytes

Nickel (mg dm^{-3})	$[BMIM]HSO_4$ (mg dm^{-3})	Current efficiency (%)	Cathodic contamination (%)	Crystallographic orientation
1	0	90.5	–	(101) (100) (102) (103)
2	0	90.1	–	–
5	0	82.9	–	(101) (102) (103) (112)
10	0	76.8	0.029	(101) (102) (103) (112)
20	0	59.9	0.027	(101) (102) (002) (100)
10	5	87.3	–	(101) (100) (102) (112)
10	10	88.2	–	(101) (102) (112) (100)

Table 4 Effects of $[BMIM]HSO_4$ on current efficiency, cathodic contamination, and crystallographic orientations of the zinc electrodeposits obtained from cobalt-containing electrolytes

Cobalt (mg dm^{-3})	$[BMIM]HSO_4$ (mg dm^{-3})	Current efficiency (%)	Cathodic contamination (%)	Crystallographic orientation
1	0	90.6	–	(101) (112) (102)
2	0	90.0	–	–
5	0	89.7	–	(101) (102) (110) (112)
10	0	89.1	0.016	(101) (100) (110) (112)
20	0	82.0	0.017	(101) (100) (110) (112)
10	5	90.4	–	(101) (102) (112) (103)
10	10	91.0	–	(101) (100) (110) (102)

Table 5 Effects of $[BMIM]HSO_4$ on current efficiency, cathodic contamination, and crystallographic orientations of the zinc electrodeposits obtained from lead-containing electrolytes

Lead (mg dm^{-3})	$[BMIM]HSO_4$ (mg dm^{-3})	Current efficiency (%)	Cathodic contamination (%)	Crystallographic orientation
1	0	91.1	0.019	(101) (112) (100)
2	0	91.2	0.035	–
5	0	91.6	0.086	(101) (110) (102) (002)
10	0	92.0	0.161	(101) (100) (002)
20	0	91.7	0.318	–
10	5	89.1	0.091	(101) (102) (100)
10	10	89.8	0.040	(101) (102) (100) (103)

electrodeposited nickel or cobalt sites act as local cathodes for hydrogen evolution, and the adjacent zinc sites act as local anodes for zinc dissolution. However, by virtue of their being a kind of electronegative metals, the electrodeposited nickel and cobalt will redissolve in the acidic electrolyte, and then co-deposit with zinc on the cathode again. These deposition–dissolution cycles allow them having more pronounced effect on the CE than other impurities with a low concentration in the deposits. Ionic liquid additive $[BMIM]HSO_4$ is found to relieve the

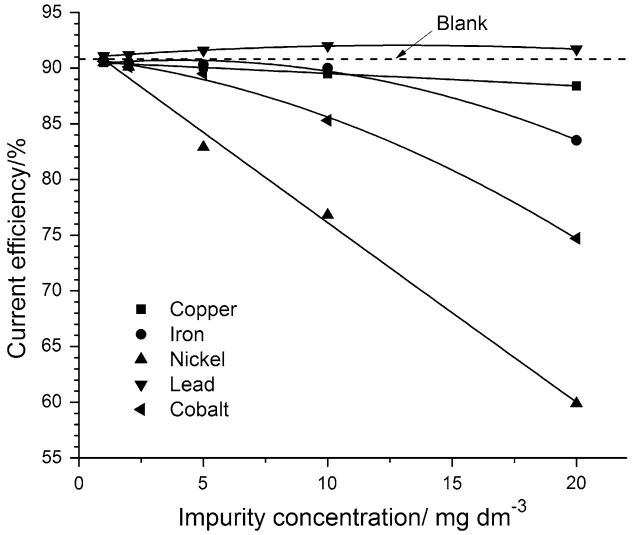

Fig. 1 The effect of various impurities on the current efficiency during zinc electrodeposition

harmful effects of these impurities to some extent where the degree of contamination of these impurities in the zinc deposits is reduced, and this observation is consistent with the discussion in the previous section. Addition of 5 mg dm^{-3} [BMIM]HSO_4 to the electrolyte containing 10 mg dm^{-3} copper, the copper content in the zinc deposit reduces by $\sim$0.120% in comparison to the additive-free electrolyte. Similar change trends of the contamination in the zinc deposits are also observed with the addition of [BMIM]HSO_4 in the other impurity-containing electrolytes. This is attributed to the adsorption of [BMIM]HSO_4 on the active sites of the electrode surface, which restricts these impurities ions from being adsorbed on the cathodic electrode surface and electroreduced, thereby reducing their content in the zinc deposits.

3.3 Surface morphology

The typical scanning electron micrographs for the zinc deposits obtained from the impurity-containing electrolytes in the absence and presence of [BMIM]HSO_4 are shown in Figs. 2, 3, 4, 5, and 6. As can be seen, the investigated impurities induce some changes in the morphology of the zinc deposits as compared with those obtained from pure zinc sulfate solution, and the differences among the various types of deposits are often quite profound.

The zinc deposit obtained from additive/impurity-free solution is bright, but not smooth and consisted of hexagonal platelets of moderate size (Fig. 2a) as discussed in our pervious study [20]. The deposit obtained from copper-containing electrolyte gives a dull and dark deposit with decreasing grain size (Fig. 2b). This effect is more pronounced with the increase in copper concentration

Table 6 The standard reduction electrode potential

Electrode process	Standard electrode potential vs. SCE (V)
$Zn^{2+} + 2e^- \rightarrow Zn$	$E^0 = -1.002$
$Fe^{2+} + 2e^- \rightarrow Fe$	$E^0 = -0.687$
$Fe^{3+} + 3e^- \rightarrow Fe$	$E^0 = -0.277$
$Fe^{3+} + e^- \rightarrow Fe^{2+}$	$E^0 = -0.531$
$Co^{2+} + 2e^- \rightarrow Co$	$E^0 = -0.520$
$Ni^{2+} + 2e^- \rightarrow Ni$	$E^0 = -0.497$
$Pb^{2+} + 2e^- \rightarrow Pb$	$E^0 = -0.366$
$Cu^{2+} + e^- \rightarrow Cu^+$	$E^0 = -0.087$
$Cu^+ + e^- \rightarrow Cu$	$E^0 = -0.281$
$Cu^{2+} + 2e^- \rightarrow Cu$	$E^0 = -0.102$
$2H^{2+} + 2e^- \rightarrow H_2$	$E^0 = -0.240$

(Fig. 2c). This can be explained by the fact that copper is reduced to the metallic state, electrolytically, before zinc and co-deposit with it. Addition of 5 mg dm^{-3} [BMIM]HSO_4 to the solution containing 10 mg dm^{-3} copper leads to more smooth and uniform deposit with a further decrease in the size of the crystallites (Fig. 2d). The grain refinement shows clearly that an inhibition of the electrocrystallization process took place. The action of [BMIM]HSO_4 is one of inhibition of the crystal growth process through its cathodic adsorption, so that a relative enhancement of the nucleation process is induced. This results in a finer-grained deposit.

Iron is found to have a pronounced effect on the morphology of the electrodeposited zinc similar to copper. The addition of 5 mg dm^{-3} iron produces a compact deposit with pyramidal growth of crystallites (Fig. 3a). Increasing the concentration to 10 mg dm^{-3} causes the crystallites to grow in the form of irregular distribution (Fig. 3b). Combined addition of 5 mg dm^{-3} [BMIM]HSO_4 and 10 mg dm^{-3} iron results in more compact deposit with all the crystals distributing uniformly on the surface (Fig. 3c). With further increase in the concentration of [BMIM]HSO_4 to 10 mg dm^{-3} (Fig. 3d), the deposit obtained appears to be more compact and fine-grained.

Coarse crystalline deposit of button-like dendrites with irregular distribution is obtained in the electrolyte containing 10 mg dm^{-3} nickel (Fig. 4b). Addition of 5 mg dm^{-3} [BMIM]HSO_4 in the electrolyte results in the crystallites growing in the form of regular shape throughout the surface (Fig. 4c). Further increase in the concentration of [BMIM]HSO_4 to 10 mg dm^{-3} produces more compact and grain-refining deposit (Fig. 4d).

Both cobalt and lead have a similar effect on the physical appearance of the zinc deposits, making the deposit surface become rougher and appear with slightly increased platelet size at higher additive concentration

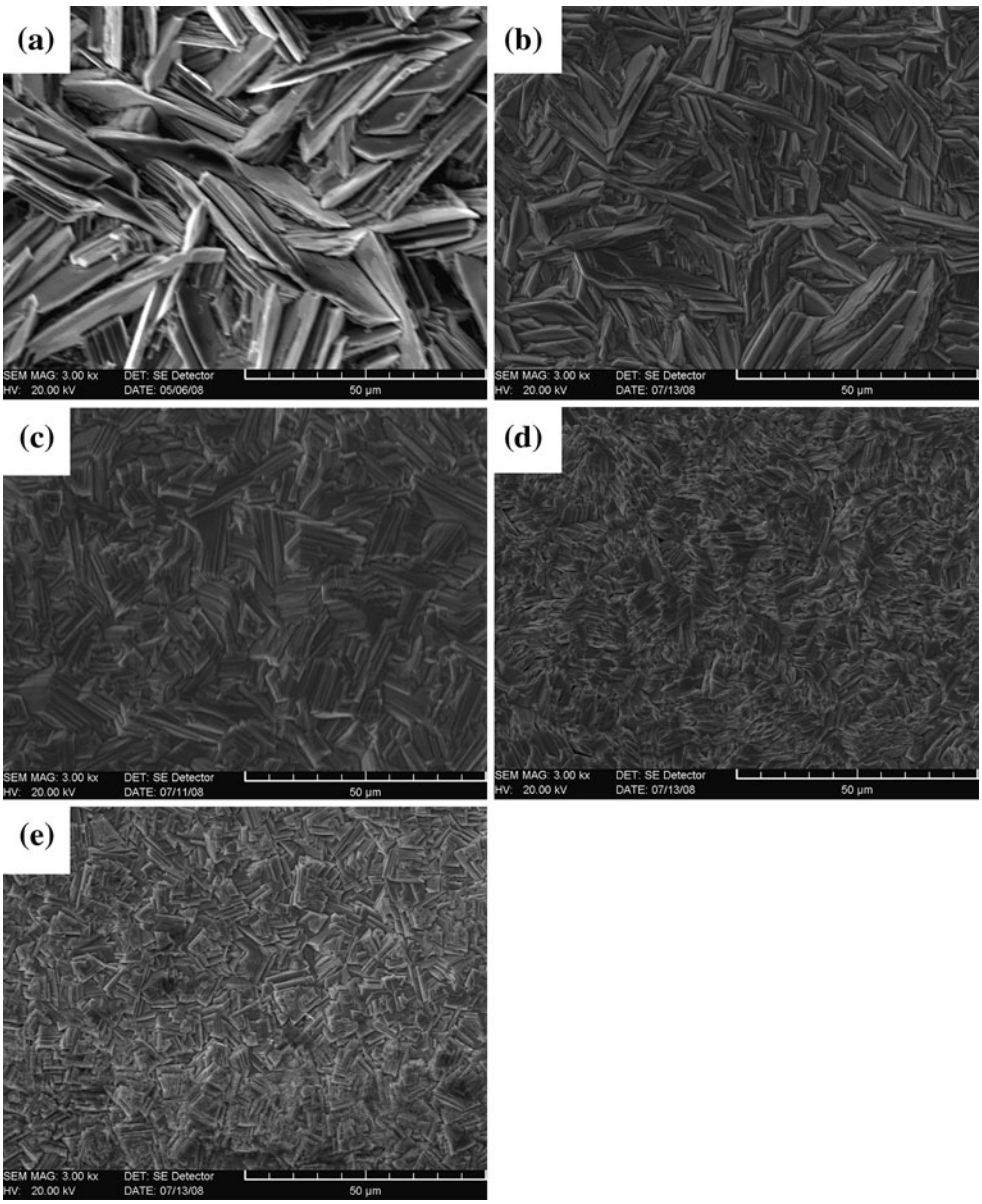

Fig. 2 Scanning electron micrographs of the zinc electrodeposits obtained from copper-containing electrolytes in the absence and presence of $[BMIM]HSO_4$. (a) Blank, (b) 5 mg dm^{-3} copper, (c) 10 mg dm^{-3} copper, (d) [c] + 5 mg dm^{-3} $[BMIM]HSO_4$, (e) [c] + 10 mg dm^{-3} $[BMIM]HSO_4$

(Figs. 5b, 6b) in comparison to the cases at lower concentration (Figs. 5a, 6a). Simultaneously, a major reduction in the size of the zinc crystals (grain-refining) and a much more compact deposit are obtained when $[BMIM]HSO_4$ is also present in the electrolyte. In the case of cobalt, the combination of 5 mg dm^{-3} $[BMIM]HSO_4$ and 10 mg dm^{-3} cobalt markedly decreases the size of zinc crystals (Fig. 5c). Increasing the $[BMIM]HSO_4$ concentration to 10 mg dm^{-3} results in a similar but more compact morphology (Fig. 5d). In the case of lead, a progressive decrease in the grain size of the zinc crystals is obtained by increasing the concentration of $[BMIM]HSO_4$ from 5 to 10 mg dm^{-3} in the electrolyte containing 10 mg dm^{-3} lead (Fig. 6c, d).

3.4 Crystallograhic orientation

The effects of $[BMIM]HSO_4$ on the crystallographic orientations of electrodeposited zinc obtained from impurity-containing electrolytes were examined using X-ray diffraction, and the results are presented in Tables 1, 2, 3, 4, and 5. The order of preferred crystal orientations for the deposit obtained from additive/impurity-free zinc electrolyte is (101), (201), (100), (112) (Table 1). The initial addition of copper (2 mg dm^{-3}) abruptly changes the crystallographic orientations of zinc deposit with the growth of (103), (102), and (100) crystal planes. The order of preferred crystal orientations for it at this concentration is (101), (103), (102), (100). Addition of 5 mg dm^{-3}

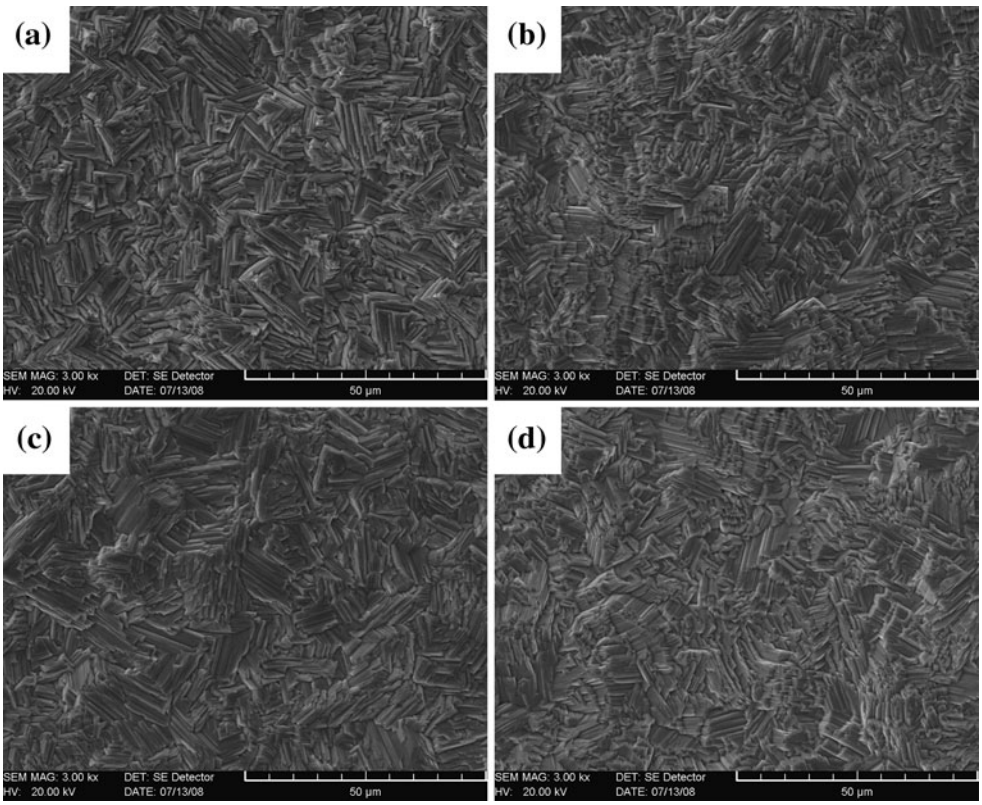

Fig. 3 Scanning electron micrographs of the zinc electrodeposits obtained from iron-containing electrolytes in the absence and presence of $[BMIM]HSO_4$. (a) 5 mg dm^{-3} iron, (b) 10 mg dm^{-3} iron, (c) [b] + 5 mg dm^{-3} $[BMIM]HSO_4$, (d) [b] + 10 mg dm^{-3} $[BMIM]HSO_4$

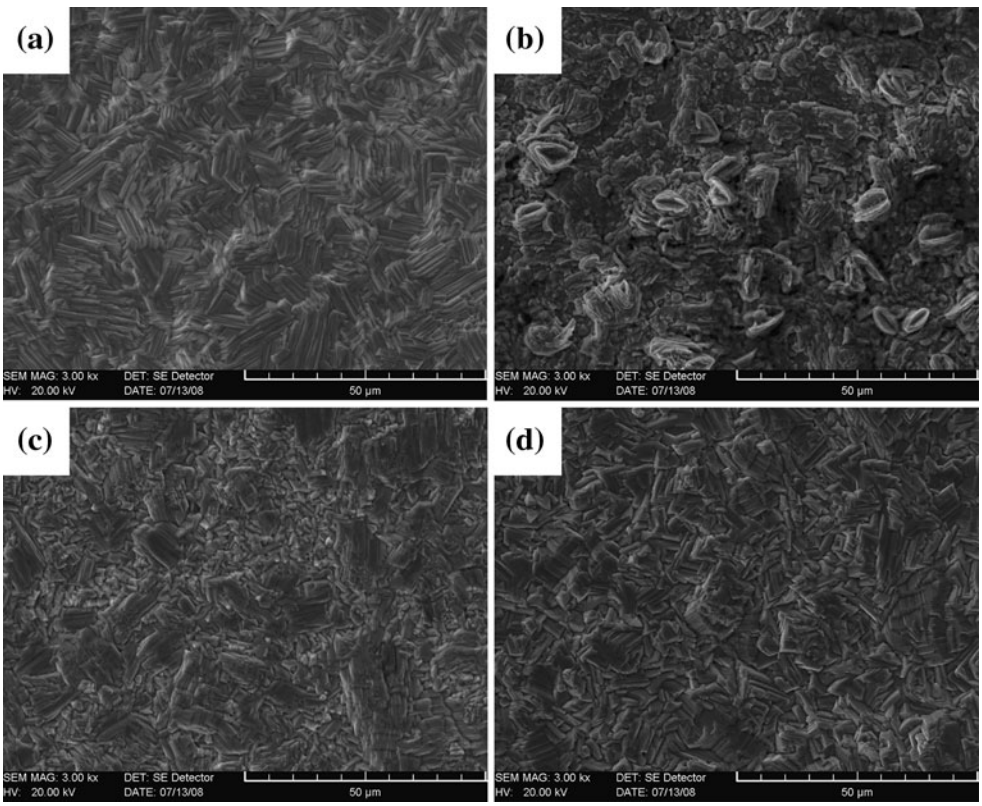

Fig. 4 Scanning electron micrographs of the zinc electrodeposits obtained from nickel-containing electrolytes in the absence and presence of $[BMIM]HSO_4$. (a) 5 mg dm^{-3} nickel, (b) 10 mg dm^{-3} nickel, (c) [b] + 5 mg dm^{-3} $[BMIM]HSO_4$, (d) [b] + 10 mg dm^{-3} $[BMIM]HSO_4$

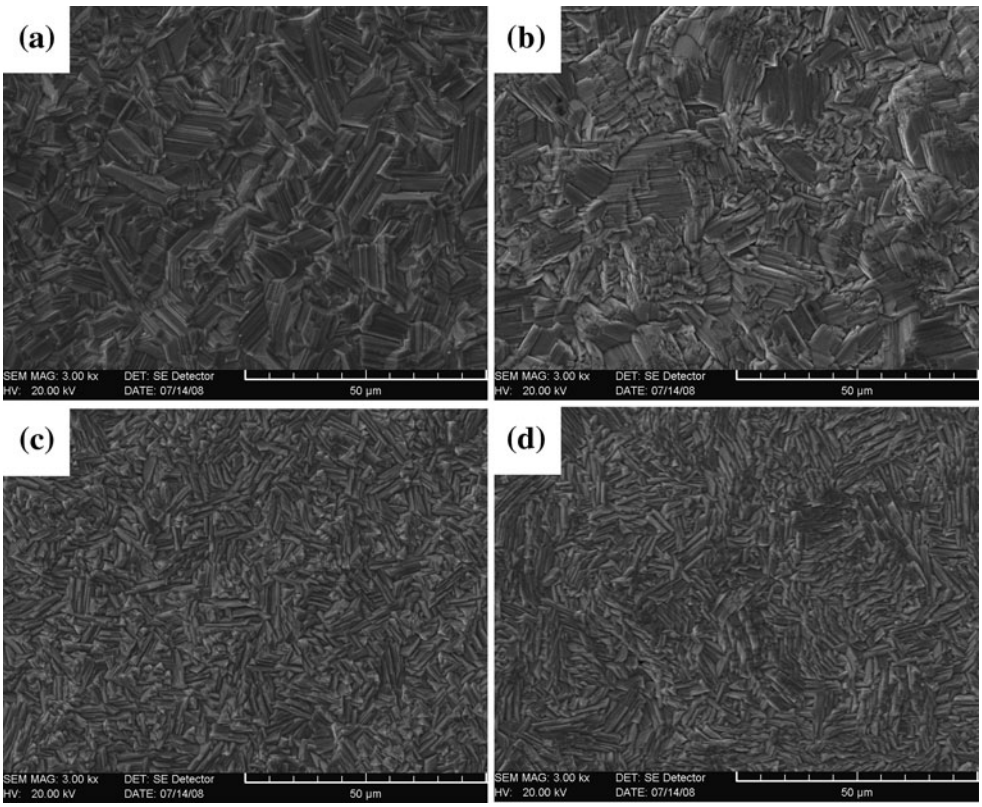

Fig. 5 Scanning electron micrographs of the zinc electrodeposits obtained from cobalt-containing electrolytes in the absence and presence of $[BMIM]HSO_4$. (a) 5 mg dm^{-3} cobalt, (b) 10 mg dm^{-3} cobalt, (c) [b] + 5 mg dm^{-3} $[BMIM]HSO_4$, (d) [b] + 10 mg dm^{-3} $[BMIM]HSO_4$

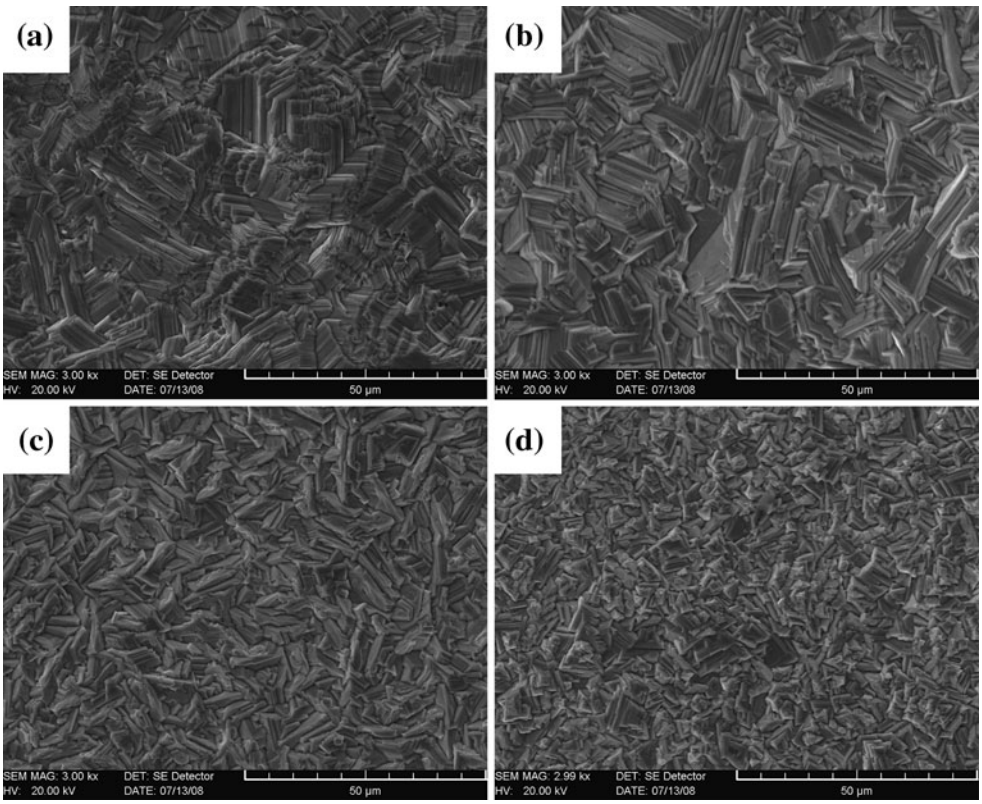

Fig. 6 Scanning electron micrographs of the zinc electrodeposits obtained from lead-containing electrolytes in the absence and presence of $[BMIM]HSO_4$. (a) 5 mg dm^{-3} lead, (b) 10 mg dm^{-3} lead, (c) [b] + 5 mg dm^{-3} $[BMIM]HSO_4$, (d) [b] + 10 mg dm^{-3} $[BMIM]HSO_4$

copper does not change the preferred crystal orientation pattern. Further increase in the copper concentration to 10 mg dm^{-3} causes a significant fall in the peak intensity of (103) crystal plane and results in (101), (002), (100), and (110) as the preferred orientations. With the combination of 5 mg dm^{-3} [BMIM]HSO_4 and 10 mg dm^{-3} copper, the order of the preferred orientations is (101), (002), (100), (103). However, when the concentration of [BMIM]HSO_4 is increased to 10 mg dm^{-3}, the crystallite growth in the direction of (100) and (002) planes are inhibited, and the order changes to (101), (110), (102).

When zinc is deposited from the iron-containing electrolyte (Table 2), the crystallites grow predominantly in the direction of the (102) and (103) planes. Addition of 2 mg dm^{-3} iron suppresses the growth of the (100) plane and promotes the growth of the crystallites in the direction of the (102) and (103) planes. Thus, the order of preferred orientations is (101), (102), (103). An increase in the iron concentration to 10 mg dm^{-3} promotes the growth of the (112) crystal planes and results in (101), (112), (103), and (102) as the preferred orientation. In addition, the presence of [BMIM]HSO_4 in the electrolyte containing 10 mg dm^{-3} iron produces slightly different crystal orientation pattern. At the concentration of 5 mg dm^{-3}, the growth of (100) plane is promoted. Increasing the concentration to 10 mg dm^{-3}, the degree of (103) and (100) planes decreases, and the order of the preferred plane is changed to (101), (102), (112), (103).

The electrodeposits obtained from the nickel-containing solution show crystal growth in the (102) and (103) directions similar to the deposits obtained from the iron-containing solution (Table 3). However, the growth in the (102) plane is found to be more favored in the case of the former. Addition of 1 mg dm^{-3} nickel changes the order of the crystal pattern to (101), (100), (102), (103). An increase in nickel concentration from 5 to 10 mg dm^{-3} does not change the order of the preferred orientations. However, growth in the direction of the (100) plane is suppressed. The combination of 5 mg dm^{-3} [BMIM]HSO_4 and 10 mg dm^{-3} nickel exhibits a (101), (100), (102), (112) preferred orientation. Further increase in the concentration of [BMIM]HSO_4 to 10 mg dm^{-3} does not change the preferred crystal planes but varies the order to (101), (102), (112), (100).

The preferred crystal orientations of the zinc deposit obtained from cobalt-containing solution produces slightly different crystal orientations (Table 4). With the addition of 1 mg dm^{-3}, the order of preferred crystal orientation is (101). (112). (102), whereas with that of 5 mg dm^{-3} cobalt, the order of preferred crystal orientations changes to (101), (102), (110), (112). Further increase in the concentration of cobalt does not change the preferred orientation of (101), (100), (110), (112). The simultaneous presence of 10 mg dm^{-3} cobalt and [BMIM]HSO_4 changes the preferred orientations to (101), (102), (112), (103) for 5 mg dm^{-3} [BMIM]HSO_4, and (101), (100), (110), (102) for 10 mg dm^{-3} [BMIM]HSO_4.

The presence of lead in the electrolyte promotes the crystal growth in the direction of the (100) plane (Table 5). Addition of 1 mg dm^{-3} lead changes the order of the crystal pattern to (101), (112), (100). An increase in the concentration of lead to 10 mg dm^{-3} increases the peak intensities of the (100) and (002) planes, thus favoring growth in these directions. A similar observation is also reported by Mackinnon et al. [13] who observed that increasing lead concentration in the zinc deposits progressively changed the orientations from (112) to (101) to (100) to finally a poorly shaped crystalline (002) structure. The crystal orientation is changed from (101), (100), and (002), as major planes for 10 mg dm^{-3} lead to an orientation dominated by the (101), (102), and (100) planes for combined addition of 5 mg dm^{-3} [BMIM]HSO_4. When the [BMIM]HSO_4 concentration increases up to 10 mg dm^{-3}, the growth of a new (103) plane is obtained. It is interesting to note that in all the cases, (101) plane remains as the most preferred plane. Moreover, these marked changes in the crystallographic orientations are also reflected in the deposits' morphology.

4 Conclusions

The effects of ionic liquid additive [BMIM]HSO_4 on the CE, surface morphology, and crystallographic orientations during zinc electrodeposition from acidic sulfate solutions containing various impurities such as copper, iron, cobalt, nickel, and lead have been investigated, and the conclusions drawn from the results are summarized as follows:

(1) All the impurities studied exert a deleterious effect on CE except Pb and their negative influence on CE is in the order: Ni > Co > Cu > Fe > Pb. Addition of [BMIM]HSO_4 to the copper, iron, cobalt, and nickel-containing electrolytes increase the CE by ~1–11% compared to those obtained from the impurity-containing alone solutions; however, a decrease in CE by ~2% is obtained in the case of Pb.

(2) All the zinc deposits are found to be contaminated in the presence of impurities, and their contents in the deposits increase with increasing impurity concentration in the electrolytes. The extent of contamination of the zinc deposits in the presence of these impurities appears to be in the order: Cu > Pb > Fe > Ni > Co. [BMIM]HSO_4 is found to relieve the harmful effects of these impurities to some extent that leads to reduction in the contents of these impurities in cathodic deposits.

(3) The investigated impurities induce some changes in the morphology of the zinc deposits, and the differences among the various types of deposits are quite profound. Addition of appropriate amounts of $[BMIM]HSO_4$ to the impurity-containing electrolytes produces smoother, more leveled, and fine-grained cathodic deposits.

(4) In the range of study, impurities alone and in combination with $[BMIM]HSO_4$ do not change the structure of the electrodeposited zinc but affect the preferred crystallographic orientations of the crystal planes. In all the cases, the (101) plane is found to be the most preferred crystal plane.

Acknowledgments The authors thank XinSheng Li for assistance in SEM and gratefully acknowledge the financial support of the National Natural Science Foundation of China (Projects No. 50864009 and 50904031), and the Research Fund for the Doctoral Program of Higher Education of China (Project No. 20070674001).

References

1. Robinson DJ, O'Keefe TJ (1976) J Appl Electrochem 6:1
2. MacKinnon DJ, Brannen JM (1977) J Appl Electrochem 7:451
3. Lamping BA, O'Keefe TJ (1976) Metall Trans 7B:551
4. Mackinnon DJ (1985) J Appl Electrochem 15:953
5. Mackinnon DJ, Brannen JM, Fenn PL (1987) J Appl Electrochem 17:1129
6. Maja M, Spinelli P (1971) J Electrochem Soc 118:1538
7. Muresan L, Maurin G, Oniciu L, Gaga D (1996) Hydrometallurgy 43:345
8. Saba AE, Elsherief AE (2000) Hydrometallurgy 54:91
9. Wark IW (1979) J Appl Electrochem 9:721
10. Maja M, Penazzi N, Fratesi R, Roventi G (1982) J Electrochem Soc 129:2695
11. Mackinnon DJ, Morrison RM, Brannen JM (1986) J Appl Electrochem 16:53
12. Stefanov Y, Vane I (2002) Hydrometallurgy 64:193
13. Mackinnon DJ, Brannen JM, Kerby RC (1979) J Appl Electrochem 9:55
14. Fosnacht DR, O'Keefe TJ (1980) J Appl Electrochem 10:495
15. Mackinnon DJ, Fenn PL (1984) J Appl Electrochem 14:467
16. Mackinnon DJ, Fenn PL (1984) J Appl Electrochem 14:701
17. Fosnacht DR, O'Keefe TJ (1983) Metall Trans 14B:645
18. Ault AR, Frazer EJ (1988) J Appl Electrochem 18:583
19. Tripathy BC, Das SC, Singh P, Hefter GT, Misra VN (2004) J Electroanal Chem 565:49
20. Zhang QB, Hua YX (2009) J Appl Electrochem 39:261
21. Sato R (1959) J Electrochem Soc 106:206
22. Hosny AY (1993) Hydrometallurgy 32:261
23. Karavasteva M, Kraivanov St (1993) J Appl Electrochem 23:763
24. Sider M, Piron DL (1988) J Appl Electrochem 18:54
25. Cachet C, Wiart R, Ivanov I, Stefanov Y, Rashkov S (1994) J Appl Electrochem 24:71
26. Karavasteva M (1994) Hydrometallurgy 35:391
27. Das SC, Singh P, Hefter GT (1996) J Appl Electrochem 26:1245
28. Das SC, Singh P, Hefter GT (1997) J Appl Electrochem 27:738
29. Tripathy BC, Das SC, Singh P, Hefter GT (1997) J Appl Electrochem 27:673
30. Tripathy BC, Das SC, Hefter GT, Singh P (1998) J Appl Electrochem 28:915
31. Tripathy BC, Das SC, Singh P, Hefter GT (1999) J Appl Electrochem 29:1229
32. Tripathy BC, Das SC, Misra VN (2003) Hydrometallurgy 69:81
33. Whitehead JA, Lawrance GA, McCluskey A (2004) Aust J Chem 57:151
34. Zhang QB, Hua YX, Yan Li, Pei QF (2009) J Appl Electrochem 39:2329